Spectral dependence of light output from LEIT devices on electrode morphology

1989 J. Phys.: Condens. Matter 1 7931

(http://iopscience.iop.org/0953-8984/1/42/014)

J. Phys.: Condens. Matter 1 (1989) 7931–7940. Printed in the UK

Spectral dependence of light output from LEIT devices on electrode morphology

A J L Ferguson, D G Walmsley, H P Hagan, R J Turner and P Dawson
Department of Pure and Applied Physics, Queen's University, Belfast BT7 1NN, UK

Received 3 March 1989, in final form 20 July 1989

Abstract. The light output from Al–I–Au tunnel junctions is observed to depend on the morphology of the Au film electrode. Films deposited quickly (2 nm s^{-1}) give out less light, especially towards the blue end of the spectrum, than those deposited slowly (0.03 nm s^{-1}). An explanation is offered in terms of elastic scattering of surface plasmon polaritons in the Au film. The scattering increases the chance of plasmon decay by internal electromagnetic absorption at the expense of photon emission. A model, of more general applicability, has been developed which can explain the results. SEM has been used to determine the grain size in the Au films and STM to measure the surface roughness.

1. Introduction

For a number of years there has been interest in the emission of light from tunnel junctions, so-called light emission by inelastic tunnelling (LEIT). Its spectral form is surprisingly inconsistent from one investigation to another and there have been suggestions (Kirtley *et al* 1981, Kroo *et al* 1986) that variations in electrode morphology may be at the root of the problem. In the present study we have combined spectral measurements with determinations of electrode topography by scanning tunnelling microscopy (STM) and SEM studies of grain size to explore the issue. A model of the light emission process is developed to assist in interpreting the results.

Thin-film metal–insulator–metal tunnel sandwiches emit broad-band light up to a maximum frequency, ν_0, when a DC bias, V_0, is applied between the metal electrodes (Lambe and McCarthy 1976). A quantum condition

$$h\nu_0 = eV_0$$

determines the maximum output frequency. The present physical understanding is that fluctuations (shot noise) in the tunnel current with a power spectrum

$$\langle I_\omega^2 \rangle = eI_0(1 - h\nu/eV_0) \qquad h\nu < eV_0$$

$$\langle I_\omega^2 \rangle = 0 \qquad h\nu > eV_0$$

where I_0 is the DC current under bias, V_0, excite surface plasmon polaritons (SPPs) in the electrodes and these decay by the emission of photons at the electrode surfaces. Because SPPs propagate at less than the speed of light it is impossible to conserve both energy and momentum during the emission process at a smooth surface. In practice, most metal surfaces are sufficiently rough to provide the necessary coupling between SPPs of

0953-8984/89/427931 + 10 $02.50

wavevector k_{sp}, and photons of wavevector k, via the reciprocal of the surface roughness correlation length λ_r:

$$k_{sp} = k \sin \theta + 2\pi/\lambda_r.$$

Here θ is the angle of photon emission relative to the mean surface normal. Light is therefore emitted if the surface is naturally rough. The intensity is increased if deliberate roughening is introduced. The roughening can be achieved by chemically etching the outermost surface (Lambe and McCarthy 1976) or by depositing the film sandwich on a rough substrate which has the effect of making all the interfaces rough as well. Common practice has been to use either diffraction gratings (Kroo *et al* 1981, Kirtley *et al* 1981) or microcrystalline films of materials such as CaF_2 (McCarthy and Lambe 1977) as substrates.

Some progress has been made towards understanding the variation of the emitted light intensity with angle and frequency. A theory by Laks and Mills (1979, 1980) which developed earlier ideas of Davis (1977) and Rendell *et al* (1978) has frequently been used in the interpretation of experimental results (Kirtley *et al* 1981, Dawson *et al* 1984, Moulessehoul and Septier 1984, Ushioda *et al* 1985, 1986, Kurdi and Hall 1986, Donohue and Wang 1986, Kroo *et al* 1986, Soole and Hughes 1988). The distribution of light intensity with *angle* seems to be reproducible from one sample to another and is in agreement with theoretical predictions (Laks and Mills 1979, 1980, Takeuchi *et al* 1988). However, there are serious discrepancies between the *spectra* reported by different research groups for nominally identical or similar samples (e.g., Parvin and Parker 1981, Dawson *et al* 1984, Donohue and Wang 1986, Watanabe *et al* 1988). We have confirmed significant irreproducibility in spectral output from one sample to another made under supposedly similar conditions. We have therefore varied the preparation conditions deliberately to see if the spectral form of the light output can be changed in a controllable way.

2. Experiment

Al–I–Au tunnel sandwiches with rough surfaces and interfaces have been prepared on glass substrates over an initial film of CaF_2, about 100 nm thick, deposited at 2 nm s^{-1}. The Al films, 50 nm thick, were deposited at 1 nm s^{-1}. The insulator resulted from air oxidation of the Al film at 100–150 °C for 5 min. Subsequently the 20 nm thick Au films were cross deposited, some at a slow (0.03 nm s^{-1}) and some at a fast (2 nm s^{-1}) rate. The samples were aged at room temperature for a period of 1 to 10 days until the resistance had increased sufficiently to develop a bias of 3 V at a test current of 20 mA. Thereafter the samples were stored in liquid nitrogen until and during the optical measurements. Each of the metal films is 7 mm wide, so the light-emitting area at their intersection is about 0.5 cm^2. Narrow (1 mm wide) Al evaporated films make contact from the ends of the films to one edge of the glass substrate. The substrate is suspended from an edge connector in a bath of liquid nitrogen during the optical measurements: the samples have a more stable resistance when operated at 77 K and a much longer life (months as opposed to hours at room temperature). The high applied electric fields (3 V across 2 nm) can sometimes cause a decrease in the resistance of the tunnel insulator during a spectral measurement (typical duration 14 minutes). This problem is overcome, if it arises, by applying a periodic short negative-bias pulse to the sample.

The topography of the films was plotted with a scanning tunnelling microscope (STM) similar to the pocket-size model introduced by Gerber *et al* (1986). For these

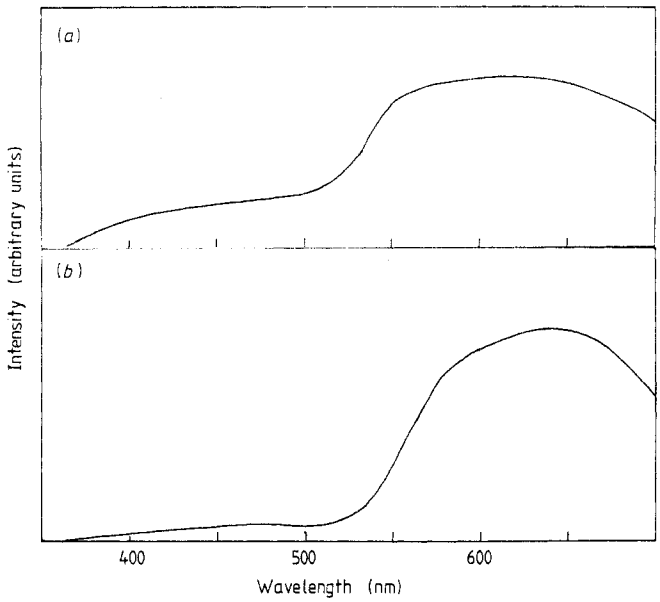

Figure 1. Emission spectra (photon count) at $\theta = 0°$ from roughened CaF_2–Al–Al_2O_3–Au tunnel junctions. (*a*) Applied bias, V_0, = 3.45 V; current, i, = 14 mA; 20 nm Au film deposited at 0.028 nm s^{-1}. (*b*) Applied bias, V_0, = 3.41 V; current, i, = 50 mA; 20 nm Au layer deposited at 2.0 nm s^{-1}.

measurements the samples were examined in air at room temperature after the optical measurements were complete. The piezoelectric arms of the STM were calibrated optically with a Newton's rings arrangement and checked against atomic structure seen in HOPG graphite.

The scanning electron microscope (SEM) pictures were taken on a Jeol JSM 840 Instrument.

3. Results

The spectral output from a slow-evaporated Au film is shown in figure 1(*a*) and from a fast-evaporated film in figure 1(*b*). Although some variations occur from one sample to another prepared under similar conditions, the suppression of output at the blue end in fast-evaporated films was consistently observed. The overall intensity was usually down at all wavelengths in fast-evaporated films—typically by a factor of 10 at the red end of the spectrum and 40–50 in the blue. The peaks in the spectra were shifted towards the red in fast-deposited films.

An SEM photograph of a slow-evaporated Au film is shown in figure 2(*a*) and of a fast-evaporated film in 2(*b*). STM topographs of slow- and fast-evaporated Au films are shown in figures 3(*a*) and (*b*). There are very great differences in detail in the STM topographs obtained at different places on the film surface. Those shown in figure 3 should be regarded merely as representative of the type of structure revealed. The field of view of the STM is limited to just over 1 μm in each direction and there is clearly a benefit in developing instrumentation to look over ranges of 10 or 100 μm. Then, the longer-range variations in texture over the surface could more usefully be displayed. In the meantime it is necessary to supplement the topographs with the statement that the

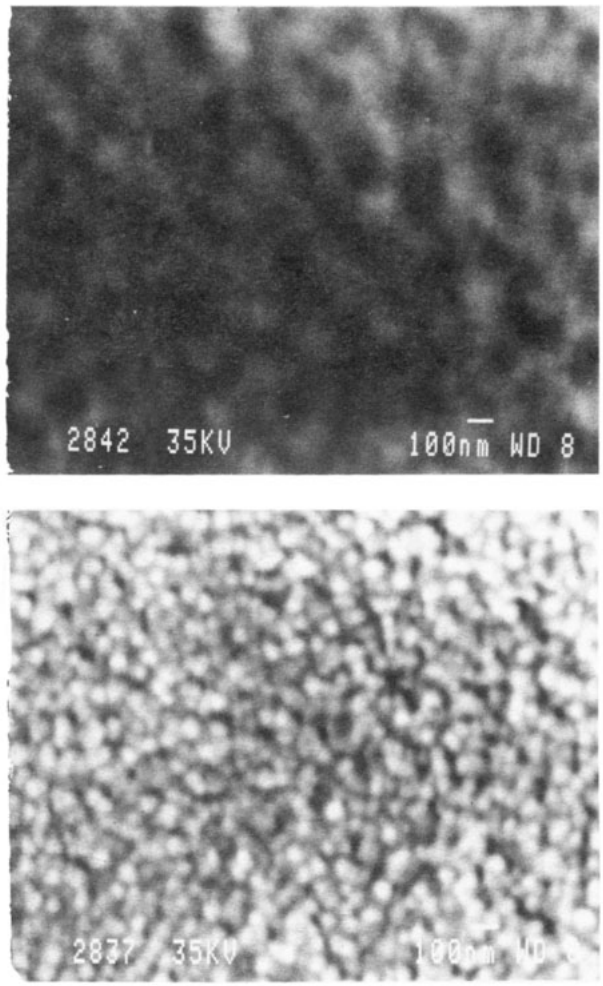

(*a*)

(*b*)

Figure 2. SEM photographs of tunnel junctions with (*a*) slow-deposited Au film and (*b*) fast-deposited Au film.

height and spacings of features observed on the surfaces are, by and large, consistent over the whole of the tunnel junction area but the detailed shapes of the features are richly varied. The STM topographs and SEM pictures were all taken in the light-emitting area of the sandwich where the Au film overlies the Al film. Out of interest we show in figure 4 an STM topograph of a weakly light-emitting Au film on top of Al but with no CaF_2 underlayer. The region in the bottom right quarter of the plot is typical of most of the film, but note that some rough regions can occur without CaF_2 underlayers. These regions are possibly important sources of the light emission from 'smooth' films.

4. Discussion

The SEM photographs show that the typical metal *grain size* in the slow-evaporated (0.03 nm s^{-1}) films is about 200 nm and in the fast-evaporated (2 nm s^{-1}) films is about 50 nm. (The underlying CaF_2 layer was deposited at the same rate, 2 nm s^{-1}, in both

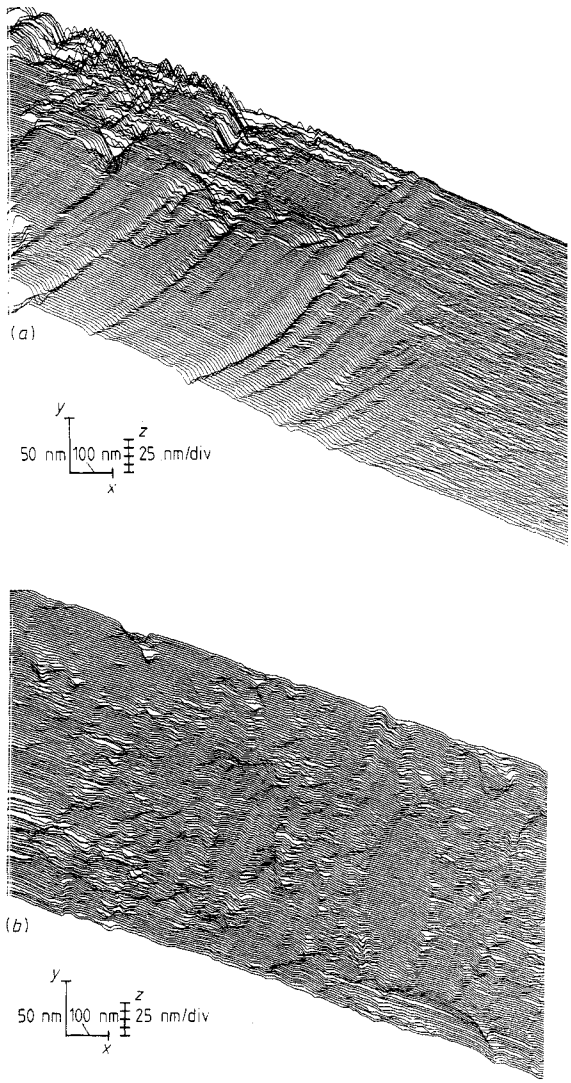

Figure 3. STM topographs of the top surface of tunnel junctions with CaF_2 underlayer: (*a*) slow-deposited Au film and (*b*) fast-deposited Au film. STM operating conditions: (*a*) tunnel voltage, $V_t = 10$ mV; tunnel current, $I_t = 7$ nA; (*b*) tunnel voltage, $V_t = 20$ mV; tunnel current, $I_t = 12$ nA.

cases.) Kroo *et al* (1986) found an average grain size of about 100 nm in Ag films deposited at an intermediate rate (0.1–1.0 nm s^{-1}).

The STM topographs in figure 3 indicate that significant *surface roughness* features, typically 25 nm high, occur at spacings of 100 ± 50 nm. STM topographs of Au films with no underlying CaF_2 layer as in figure 4 are much smoother with areas of more than 1 μm^2 having no features greater than 5 nm high.

Soole and Hughes (1988) used transmission and grazing reflection electron microscopy to determine the grain size and surface roughness of light-emitting films. In most respects their conclusions are consistent with ours. The one exception is the lateral scale of surface roughness for which they obtained 20–30 nm as against 50–150 nm here. This may be a matter of the interpretation of data from TEM versus STM. The TEM has

Figure 4. STM topograph of the top surface of a tunnel junction with no CaF_2 underlayer. The space in the middle of the plot is between two recorder sheets. STM operating conditions: tunnel voltage, $V_t = 10$ mV; tunnel current, $I_t = 8$ nA.

diffraction limitations and the STM data require further processing to allow determination of the surface profile 'power spectrum'. An attempt at such processing by Pappas *et al* (1988) suggests some agreement with the TEM work of Soole and Hughes.

An explanation of the spectral results requires a model of the light-emission process. To begin, let us suppose that the tunnelling electrons have excited SPPs at the Au–air interface. The propagation of the SPPs is influenced by three processes:

(i) electromagnetic damping in the film (a process that may include single electron-hole pair excitation through interband transitions);
(ii) decay by photon emission; and
(iii) elastic bulk scattering at grain boundaries within the film.

Electromagnetic damping can be calculated from the measured optical properties of the film metal and a propagation length, l_{em}, determined. In the case of Au, l_{em} decreases from 10 μm at 700 nm to 0.2 μm at 500 nm and remains near this value in the range 500 to 400 nm (Dawson *et al* 1984—note that the notation used there is L).

Photon emission is improbable from smooth evaporated films; light intensities from tunnel devices made without a CaF_2 underlayer are down by typically 1 or 2 orders of

magnitude from those reported here. Roughness arising from the CaF_2 underlayer is the important factor in increasing the output intensity. This roughness is revealed in the STM topographs which are particularly sensitive (~0.01 nm resolution) to the height profile of the film. The separation between surface ridges, ~100 nm, presumably mirrors the size of the CaF_2 grains.

Elastic bulk scattering of surface plasmons at grain boundaries can be expected in the films. Little attention has been paid in the literature so far to such processes. The mechanism may be envisaged as involving generation of secondary plasmons by the oscillating fringe electric fields in inter-grain gaps. It can be anticipated, like Rayleigh radiation, to be more severe at short wavelengths.

In films with large grains, elastic scattering of SPPs will be infrequent and the competition between electromagnetic damping and photon emission as SPP absorption mechanisms will be as on bulk single crystal metal surfaces. However, as the grain size in the film decreases a stage is reached when the scattering mean free path becomes comparable with or less than the separation between surface roughness features. In that situation the scattering of a SPP will *increase* the SPP path between one encounter with a *surface* roughness feature and the next. The result will be a reduced likelihood of photon emission. Electromagnetic damping per unit path length will be unchanged and the competition for SPP absorption will tilt towards internal dissipation and against photon emission. The effect may be important throughout the spectrum if elastic scattering increases with plasmon energy. Thus the basis of an explanation of the lower light output from fast-deposited films is established.

Kroo *et al* (1986) found stronger red radiation in slowly evaporated films. They recognised that structural and surface properties of the electrodes determine intensity variations from one sample to another.

Interestingly, Kirtley *et al* (1981) suspected that, for rather different reasons than discussed here, the intensity would increase with larger grain size. However, they *increased* the deposition rate from 0.2–0.4 nm s^{-1} to 1–2 nm s^{-1} to achieve greater grain size and do not report any electron microscopy data. They interpret the results in terms of tunnel electron injection mean free path rather than SPP mean free path. A frequency-independent value of 8 nm was obtained for the hot-electron mean free path.

Donohue and Wang (1986) evaporated Au at 0.3 nm s^{-1} by electron beam and found strong emission in the blue. It was attributed to *radiative plasmon* decay. No information on crystallite size was presented. The electron-beam method may heat the sample to higher temperature during preparation and give larger crystallites which would help to give greater output. We have fabricated such films on glass, and preliminary STM results show terraces with steps 10 nm high.

5. Model

A more quantitative model of how the light emission changes from films with large crystallites to those with smaller crystallites can be attempted. Suppose the mean free path of a plasmon before emission of a photon is l_{ph} and the mean free path before electromagnetic absorption within the film is l_{em}. It follows that the absolute number of emitted photons, N, will vary as l_{ph}^{-1} and competition between the two plasmon absorption processes will result in a fraction $l_{em}/(l_{em} + l_{ph})$ of the decaying plasmons following the photon emission path. Thus the number of emitted photons, N, may be written as

$$N \propto (1/l_{ph})[l_{em}/(l_{em} + l_{ph})](\nu_0 - \nu)$$

where the last term arises from the power spectrum of the exciting current. Values for

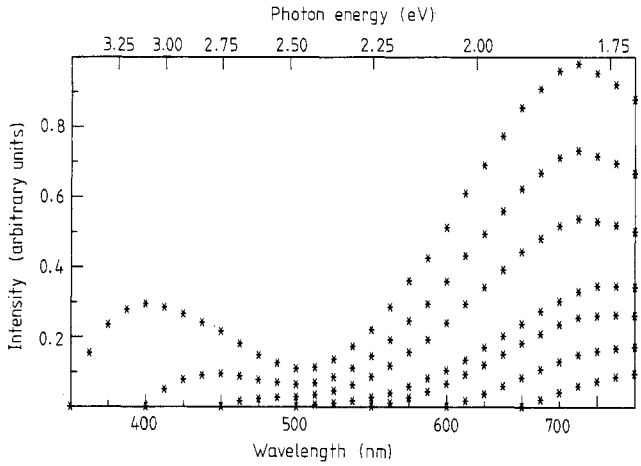

Figure 5. Plot of emitted light intensity (photon count) as function of wavelength calculated from the model described in text. No intercrystallite scattering of plasmons is assumed. The curves correspond to minimum wavelengths (maximum frequency, ν_0) cut-offs at 650, 600, 550, 500, 450, 400 and 350 nm.

l_{em} can be calculated (Dawson *et al* 1984). In the absence of knowledge about the frequency dependence of l_{ph} we assume Rayleigh-like surface scattering gives an intensity varying as ν^4. Taking account of the photon energy, $h\nu$, this implies a photon number count varying as ν^3. A similar ν^3 behaviour is to be found in the Einstein A coefficient and the expression for black body absorption by, or radiation from, an atomic dipole (Mott 1958); it is also explicitly observed as a background absorption of x-rays (by matter) on which characteristic edges from specific elements are superimposed (Agarwal 1979). We therefore put

$$l_{ph} \propto \nu^{-3}$$

As for the magnitude of l_{ph}, Moreland *et al* (1982) reported 9% efficiency for plasmon decay by photon emission in Ag films deposited on > 100 nm CaF_2 at 632.8 nm photon wavelength. Thus,

$$0.09 = l_{em}/(l_{em} + l_{ph}).$$

At this wavelength $l_{em} \simeq 47$ μm in Ag (Dawson *et al* 1984) so it follows that $l_{ph} \simeq 475$ μm. If, for simplicity, we assume $l_{ph} \gg l_{em}$ the expression for intensity simplifies to

$$N \propto \nu^6(\nu_0 - \nu)l_{em}.$$

Plots of this expression for various values of ν_0 are shown in figure 5. Remarkably, in view of its simple form, it portrays most of the important features of experimental results such as those shown in figure 1(*a*).

There remains the more general question of how the spectrum of emitted light is altered when the ratio of l_{ph} to l_{em} changes. The curves in figure 6 have been calculated from the first equation in this section without assuming $l_{ph} \gg l_{em}$. It is clear that when $l_{ph} \ll l_{em}$ there is a strong output (proportional to l_{ph}^{-1}) and little imprint of the optical constants of the Au film. At the opposite extreme, the output is dramatically reduced (and proportional to l_{ph}^{-2}) but here the effect of electromagnetic damping of the plasmon is prominent. Between these extremes can be found examples of curves that are reported in the literature for different samples. The trend from an almost featureless single high-energy maximum to a doubly peaked curve with a sharp drop in the 650–500 nm range

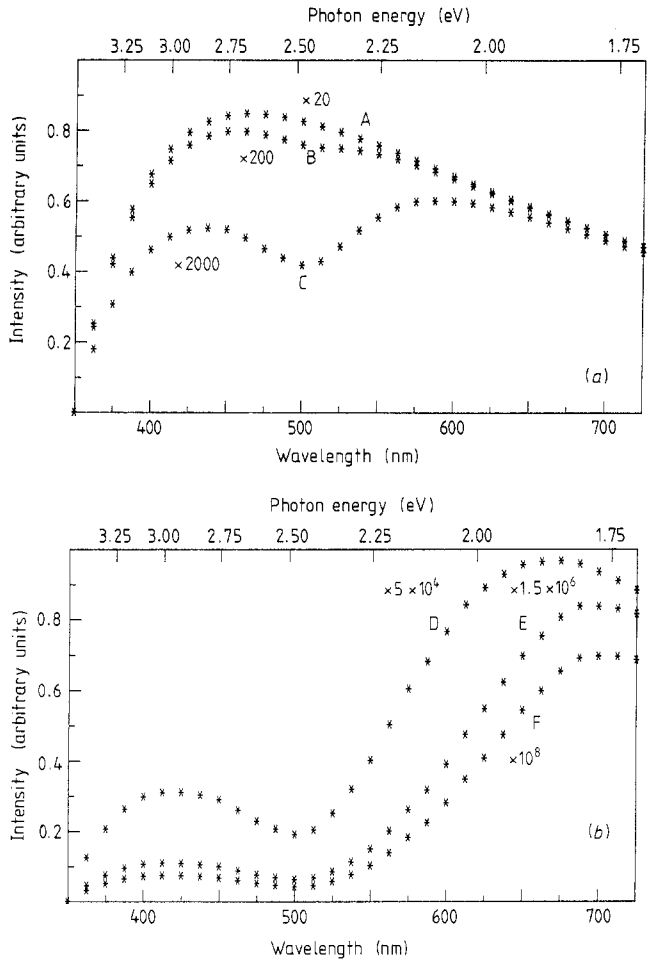

Figure 6. Plot of emitted light intensigy (photon count) as function of wavelength, calculated from model described in text, for the following values of l_{ph}/l_{em}: A, 0.01; B, 0.1; C, 1.0; D, 10; E, 100; F, 1000. For clarity, the intensities have been amplified by the values shown. In all cases the upper frequency cut-off is at 350 nm.

is smooth with increase in the ratio l_{ph}/l_{em}, i.e. with decreasing emission efficiency. The experimental results reported in figure 1(*a*) and (*b*) both appear to lie in the range $l_{ph} > l_{em}$ with the inequality more pronounced in (*b*). They roughly correspond to the calculated curves D and E of figure 6 respectively; the first of these is the regime reported by Moreland *et al* (1982) and may represent the best output that can be achieved with CaF_2 underlayers.

An alternative mechanism to elastic scattering of plasmons at grain boundaries which achieves the same effect on the ratio l_{ph}/l_{em} might be suggested: smoothing of the surface with faster film deposition. The model would then apply equally well but the STM results give no support to such an explanation.

6. Conclusions

Light-emitting tunnel junctions made with fast-evaporated Au films have a lower output intensity, especially in the blue, than similar junctions made with slow-evaporated films.

SEM studies show that the fast-deposited films have smaller grains (50 nm) than slow-deposited films (200 nm). STM topographs show that the roughness features due to the CaF_2 underlayer are typically 10 nm high and with spacings of 100 ± 50 nm. In the fast-deposited films elastic scattering increases the interval between plasmon incidences on surface roughness features and thus decreases the photon output in favour of internal damping of the plasmon. The relationship between metal grain size and the surface roughness repeat distance is important in determining the efficiency of light-emitting devices. A model of the emission process reproduces well the observations.

Acknowledgments

The authors are grateful to Professor Ushioda for preprints of his recent work which stimulated our thoughts on the present topic, and to Dr C L S Lewis for discussions.

Much of the experimental work was carried out at the University of Ulster where the encouragement of Professor G T Best, in a period of academic turmoil, was much appreciated. The assistance of Dr S Lowry in taking the SEM photographs was most valuable. Dr H P Hughes kindly supplied the HOPG graphite sample.

The support of the Science and Engineering Research Council and the Rank Prize Fund is gratefully acknowledged.

References

Agarwal B K 1979 *X-ray Spectroscopy, Springer Series in Optical Sciences* vol 15 (Berlin: Springer) p 144
Davis L C 1977 *Phys. Rev.* B **16** 2482
Dawson P, Walmsley D G, Quinn H A and Ferguson A J L 1984 *Phys. Rev.* B **30** 3164
Donohue J F and Wang E Y 1986 *J. Appl. Phys.* **59** 3137
Gerber Ch, Binnig G, Fuchs H, Marti O and Rohrer H 1986 *Rev. Sci. Instrum.* **57** 221
Kirtley J, Theis T N and Tsang J C 1981 *Phys. Rev.* B **24** 5650
Kroo N, Szentirmay Zs and Felszerfalvi J 1981 *Phys. Lett.* **81A** 399
—— 1986 *Opt. Commun.* **56** 345
Kurdi B N and Hall D G 1986 *Phys. Rev.* B **34** 3980
Laks B and Mills D L 1979 *Phys. Rev.* B **20** 4962
—— 1980 *Phys. Rev.* B **22** 5723
Lambe J and McCarthy S L 1976 *Phys. Rev. Lett.* **37** 923
McCarthy S L and Lambe J 1977 *Appl. Phys. Lett.* **30** 427
Moreland J, Adams A and Hansma P K 1982 *Phys. Rev.* B **25** 2297
Mott N F 1958 *Elements of Wave Mechanics* (Cambridge: CUP) p 132
Moulessehoul, S M and Septier A 1984 *Rev. Phys. Appl.* **19** 503
Pappas D, Sparks P D, Hopster H and Rutledge J E 1988 *Proc. STM87* ed. R M Feenstra (New York: AIP) p 415
Parvin K and Parker W 1981 *Solid State Commun.* **37** 629
Rendell R W, Scalapino D J and Muhlschlegel B 1978 *Phys. Rev. Lett.* **41** 1746
Soole J B D and Hughes H P 1988 *Surf. Sci.* **197** 250
Takeuchi A, Watanabe J, Uehara Y and Ushioda S 1988 *Phys. Rev.* B **38** 12948
Ushioda S, Rutledge J E and Pierce R M 1985 *Phys. Rev. Lett.* **54** 224
—— 1986 *Phys. Rev.* B **34** 6804
Watanabe J, Takeuchi A, Uehara Y and Ushoda S 1988 *Phys. Rev.* B **38** 12959